A Systematic Investigation on the Effects of Non-Gaussian Noise Transients and Their Mitigations to Tests of General Relativity

Jack Y. L. Kwok*
Department of Physics, The Chinese University of Hong Kong, Shatin, N.T., Hong Kong

Mentors: Alan J. Weinstein, Rico K. L. Lo
LIGO, California Institute of Technology, Pasadena, California 91125, USA
(Dated: May 31, 2020)

I. INTRODUCTION

Current gravitational-wave detectors, such as Advanced LIGO [1] and Advanced Virgo [2], are interferometers with multi-kilometer-long arms. A beam-splitter is used to split incident laser beam into two equal parts, directing them into the two arms [3]. The splitted beams are made to travel several hundred round-trips within each arm in Fabry-Pérot cavities composed of highly reflective mirrors [3]. The effective arm length is thus raised to about 1000km, optimal for the detection of gravitational waves generated by coalescing binaries with a total mass of around $1 - 100 M_\odot$ [4].

Each mirror is suspended by a system of pendulums mounted on a seismic isolation platform [5]. A gravitational wave passing through the detector is expected to change the separation of mirrors in the two arms to different extents, making the laser beams incoherent. This phase difference characterizes the light intensity of the recombined beam, which could be detected by a photodiode [3].

Aside from gravitational waves, the detected change in light intensity can be attributed to many independent sources of random noise [3]. If these noise sources are also *stationary*, i.e. their probability distributions do not change over time, the central limit theorem states that the total noise tends to be *Gaussian* when the number of noise sources is large [6]. As such, noise in gravitational-wave detectors is typically modeled to be Gaussian during data analysis [7, 8]. When signals are absent, the light intensity x received by the photodiode at each instance of time follows the Gaussian probability density

$$p(x) = \frac{1}{\sqrt{2\pi\sigma^2}} e^{-x^2/2\sigma^2} \ . \quad (1)$$

Without loss of generality, the *mean* of the distribution is set to zero. Gaussian noise is thus solely characterized by the *variance* σ^2 of the distribution. The variance could be obtained by conducting many independent experiments and calculating the mean square. Given the time series $x(t)$ in an interval $[0, T]$, we get

$$\sigma^2 = \frac{1}{T} \int_0^T x^2(t) dt \ . \quad (2)$$

It is more common to determine the variance in the frequency domain: The time series $x(t)$ is first extended to infinity by multiplying with a *window function*. The resultant time series is zero-valued outside the interval $[0, T]$ and continuous at the boundaries; it is then Fourier transformed into $\tilde{x}(f)$. Parseval's Theorem then gives

$$\sigma^2 = \frac{1}{T} \int_{-\infty}^{+\infty} x^2(t) dt = \int_0^\infty \frac{2}{T} |\tilde{x}(f)|^2 df \ . \quad (3)$$

The integrand at the right side of Eq. (3) is called the *power spectral density* (PSD). In practice, noise characteristics of a data segment of interest is estimated using the PSD of adjacent data segments [8].

The underlying assumption of stationary noise cannot account for transient, non-Gaussian noise features in gravitational-wave detectors, commonly-known as *glitches* [9–11]. Three classes of commonly-seen glitches are shown in Figure 1.

Although rare, it is possible for glitches to be present in data segments containing gravitational-wave signals; this happened during the event GW170817, in which a glitch was found to overlap the signal in the LIGO-Livingston detector [14]. Furthermore, certain noise sources such as solar events, lightning and cosmic ray showers can theoretically produce glitches in multiple detectors almost simultaneously [11], making such glitches more difficult to identify.

If the presence of glitches were not accounted for, one may infer from the detected waveform that a deviation from General Relativity (GR) has occurred. The extent to which glitches mimic the effects of a deviation of GR certainly deserve a systematic study.

II. OBJECTIVE AND METHODOLOGY

Our goal is to investigate the extent to which glitches mimic the effects of a deviation of GR, and evaluate the effectiveness of common glitch-related mitigation measures on tests of GR.

To this end, we first prepare a collection of data samples by injecting GR-consistent gravitational-wave signals onto data segments containing common and well-modeled glitches; the generating parameters of the signal, the form of glitches and the extent to which glitches overlap the signal are systematically varied in between

* Email: jackkwok@link.cuhk.edu.hk

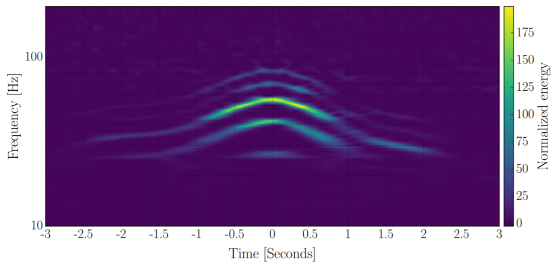

(a) A light scattering glitch [12]

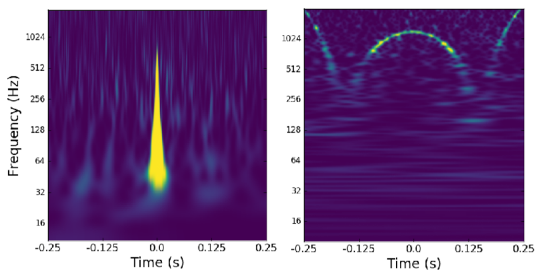

(b) A blip glitch [10] (c) A whistle glitch [10]

FIG. 1. Three normalized spectrograms of commonly-seen glitches. The colour represents the 'loudness' of the signal at each time-frequency bin [10]. (a) A light scattering glitch has a characteristic arch shape; it is caused by slight misalignments of the laser beam and the mirrors [12]. (b) A blip glitch has a characteristic 'teardrop' shape; its noise source has not been identified [13]. (c) A whistle glitch has a characteristic 'W' or 'V' shape; it is caused by radio signals generated by the interferometer control system [9].

samples. Under the assumption of Gaussian noise, we perform several identical tests of GR on each sample before and after applying mitigation measures. The former test simulates the result we would get if the existence of glitches were not accounted for; the latter tests are compared with the unmitigated case and with each other to determine the relative effectiveness of mitigation measures under different circumstances. In the following subsections, we will propose the mitigation measures, GR-consistent signal and the test of GR to be employed in our study.

A. Mitigation Measures

Many efforts are made to develop algorithms that identify glitches [15–18]; these algorithms play an important role in gravitational-wave searches. Once a glitch is identified, it could be eliminated either by hand or automatically by search pipelines [19, 20] through a process called *gating*, which zeroes out the time interval containing the glitch by multiplying the time series with an *inverse* window function [19, 20]. An example of gating is illustrated in Figure 2.

A similar procedure can be done in the frequency domain: if the glitch is localized in certain intervals of frequency, zeroing out the corresponding frequency bins would eliminate the glitch. These two procedures will henceforth be denoted as gating in the time and frequency domain respectively.

A more sophisticated approach would be to subtract off a glitch model from the original time series. This procedure, called *de-glitching*, was employed for the glitch-contaminated GW170817 data [14], as illustrated in Figure 2. The de-glitching procedure can be extended beyond well-modeled glitches using the `BayesWave` framework, which introduces a method to model glitches using wavelets and infer the most probable model using Bayesian statistics [21].

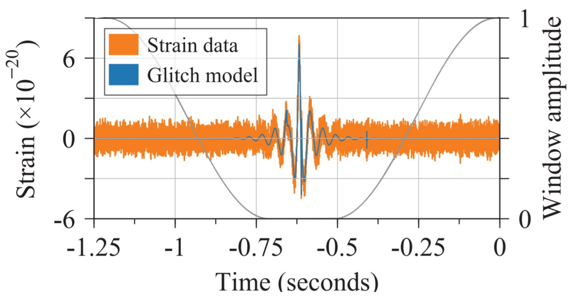

FIG. 2. The output data from the LIGO-Livingston detector during GW170817 is plotted over time (orange curve). A glitch was identified around the time $t = -0.75$s to -0.5s in the figure. To determine the sky location of the event, data was gated in the time domain by multiplying the inverse window function (black curve) [14]. To infer the source properties during parameter estimation, data was de-glitched by subtracting off a glitch model (blue curve) reconstructed with `BayesWave` [14]. The figure is retrieved from Abbott et al. [14]

In our study, we will separately apply the three standard mitigation measures of 1) gating in time domain, 2) gating in frequency domain and 3) de-glitching to data samples.

B. Injecting Signal

In GR, the two-body problem cannot be solved analytically, thus the orbital motion of coalescing binaries and the gravitational-wave signal they emit can only be computed *up to a precision*. Henceforth, an approximate waveform model predicted by GR is said to be GR-*consistent*; similarly, a signal is said to be GR-consistent if it has the exact form described by a GR-consistent waveform model.

In our study, we will use the non-spinning `TaylorF2` waveform model for its speed and agreement with numerical simulations [22]. In Fourier domain, the two polarizations $+, \times$ described by `TaylorF2` has the same phase $\Psi_{+,\times}$ but with different amplitudes $\mathcal{A}_{+,\times}$ [22].

The phase $\Psi_{+,\times}$ for various waveform models, including `TaylorF2`, can be expressed as a sum of frequencydependent terms [22, 23]. The coefficients of these terms, called the *dephasing coefficients* ψ_i, play a pivotal role in parametrized tests of GR [24], as we will show in the next subsection.

To study the relative impact of glitches on signals generated by different compact binary coalescing objects, we will systematically vary the generating parameters of the injected signal in between samples. For the non-spinning `TaylorF2` waveform model, parameters includes the time and phase of coalescence t_c, ϕ_c, the mass components, the luminosity distance D_L and the spatial configuration of the detectors during the event [22].

C. Testing GR

In this project, we will focus on a parameterized test of GR, named as the Test Infrastructure for GEneral Relativity (TIGER) [24]. This test infrastructure is chosen in our study as it does not require an alternative theory of gravity to compare against; moreover, it hinges on the measurement of parameterizable deviations, such as deviations of the dephasing coefficients from a GR-consistent waveform model [24]. We will henceforth follow the terminologies developed by Li et al. [25].

We denote $\mathcal{H}_{\mathrm{GR}}$ as the hypothesis that the gravitational-wave signal $\boldsymbol{h}$ is GR-consistent. To test against this hypothesis, we denote $\mathcal{H}_{\mathrm{modGR}}$ as the hypothesis that $\boldsymbol{h}$ has the functional form described by a GR-consistent waveform model, but differs in one or more dephasing coefficients. In practice, the deviations $\delta\chi_i$ in the dephasing coefficients ψ_i is determined up to the first order [25]:

$$\psi_i = \psi_i^{\mathrm{GR}}[1 + \delta\chi_i] \,, \tag{4}$$

where ψ_i^{GR} are the dephasing coefficients predicted by the GR-consistent waveform model. It is evident that the two hypotheses $\mathcal{H}_{\mathrm{GR}}$ and $\mathcal{H}_{\mathrm{modGR}}$ are mutually exclusive. Given data $\boldsymbol{d}$ and prior information I, we prefer the hypothesis which is relatively more probable. To quantify this statement, we can define the *odds ratio*

$$O_{\mathrm{GR}}^{\mathrm{modGR}} \equiv \frac{P(\mathcal{H}_{\mathrm{modGR}}|\boldsymbol{d}, I)}{P(\mathcal{H}_{\mathrm{GR}}|\boldsymbol{d}, I)} \,. \tag{5}$$

If the odds ratio is much greater than one, we prefer the hypothesis $\mathcal{H}_{\mathrm{modGR}}$; if it is much less than one, we prefer $\mathcal{H}_{\mathrm{GR}}$. If the odds ratio is close to 1, then the current data is inconclusive [26]. By invoking Bayes' Theorem, the odds ratio can be rewritten as

$$O_{\mathrm{GR}}^{\mathrm{modGR}} = \frac{P(\mathcal{H}_{\mathrm{modGR}}|I)}{P(\mathcal{H}_{\mathrm{GR}}|I)} \times \frac{P(\boldsymbol{d}|\mathcal{H}_{\mathrm{modGR}}, I)}{P(\boldsymbol{d}|\mathcal{H}_{\mathrm{GR}}, I)} \,. \tag{6}$$

The second term on the R.H.S. of Eq. (6) is called the *Bayes factor*, which could be readily computed with the support of Bayesian inference libraries [7, 27].

Applying the treatment of $\mathcal{H}_{\mathrm{modGR}}$ introduced in TIGER [24], we can visualize the effect of glitches on tests of GR by plotting the simulated *background distribution*, defined as the probability density of the odds ratio $\mathcal{O}_{\mathrm{GR}}^{\mathrm{modGR}}$ [25], for each data sample before mitigation. The background distributions after applying different mitigation measures will also be plotted and compared; we wish to determine the most effective mitigation measure for different degrees of glitch overlapping and different source properties of the gravitational-wave signal. A schematic plot of the background distribution for a GR-consistent signal in Gaussian noise is shown in Figure 3.

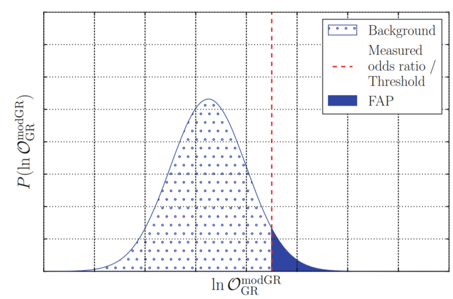

FIG. 3. The background distribution (region under blue curve) is plotted for a collection of simulated GR-consistent signals in Gaussian noise. Deviations of GR with odds ratio higher than a defined *threshold* (red dotted line) are vetoed; the threshold can be set as the odds ratio obtained for the collection of detected gravitational-wave signals. The *false alarm probability* (shaded region), defined as the probability of obtaining a odds ratio above the threshold, is shown to be an invariant quantity under choices of prior during hypothesis testing [25]. This figure is retrieved from Li [25].

III. TIMELINE

16 / 06 - 28 / 06:	Run TIGER on simulated data (without glitch)
29 / 06 - 12 / 07:	Study data **First Interim Report** Run TIGER on glitched data
13 / 07 - 26 / 07:	Visualize and summarize first batch of results
27 / 07 - 09 / 08:	**Second Interim Report** Visualize and summarize all results
10 / 08 - 21 / 08:	**Presentation, Final Report**

[1] J. Aasi, B. Abbott, R. Abbott, T. Abbott, M. Abernathy, K. Ackley, C. Adams, T. Adams, P. Addesso, R. Adhikari, *et al.*, Classical and quantum gravity **32**, 074001 (2015), arXiv:1411.4547.

[2] F. Acernese, M. Agathos, K. Agatsuma, D. Aisa, N. Allemandou, A. Allocca, J. Amarni, P. Astone, G. Balestri, G. Ballardin, *et al.*, Classical and Quantum Gravity **32**, 024001 (2014), arXiv:1408.3978.

[3] P. R. Saulson, *Fundamentals of interferometric gravitational wave detectors* (World Scientific, 1994).

[4] K. S. Thorne, S. Hawking, and W. Israel, 300 years of gravitation (1987).

[5] F. Matichard, B. Lantz, R. Mittleman, K. Mason, J. Kissel, B. Abbott, S. Biscans, J. McIver, R. Abbott, S. Abbott, *et al.*, Classical and Quantum Gravity **32**, 185003 (2015), arXiv:1502.06300.

[6] W. B. Davenport, W. L. Root, *et al.*, *An introduction to the theory of random signals and noise*, Vol. 159 (McGraw-Hill New York, 1958).

[7] LIGO Scientific Collaboration, LIGO Algorithm Library - LALSuite, free software (GPL) (2018).

[8] J. Veitch, V. Raymond, B. Farr, W. Farr, P. Graff, S. Vitale, B. Aylott, K. Blackburn, N. Christensen, M. Coughlin, *et al.*, Physical Review D **91**, 042003 (2015), arXiv:1409.7215.

[9] L. K. Nuttall, T. Massinger, J. Areeda, J. Betzwieser, S. Dwyer, A. Effler, R. Fisher, P. Fritschel, J. Kissel, A. Lundgren, *et al.*, Classical and Quantum Gravity **32**, 245005 (2015), arXiv:1508.07316.

[10] M. Zevin, S. Coughlin, S. Bahaadini, E. Besler, N. Rohani, S. Allen, M. Cabero, K. Crowston, A. K. Katsaggelos, S. L. Larson, *et al.*, Classical and Quantum Gravity **34**, 064003 (2017), arXiv:1611.04596.

[11] B. P. Abbott, R. Abbott, T. Abbott, M. Abernathy, F. Acernese, K. Ackley, M. Adamo, C. Adams, T. Adams, P. Addesso, *et al.*, Classical and Quantum Gravity **33**, 134001 (2016), arXiv:1602.03844.

[12] L. Nuttall, Philosophical Transactions of the Royal Society A: Mathematical, Physical and Engineering Sciences **376**, 20170286 (2018), arXiv:1804.07592.

[13] M. Cabero, A. Lundgren, A. H. Nitz, T. Dent, D. Barker, E. Goetz, J. S. Kissel, L. K. Nuttall, P. Schale, R. Schofield, *et al.*, Classical and Quantum Gravity **36**, 155010 (2019), arXiv:1901.05093.

[14] B. P. Abbott, R. Abbott, T. Abbott, F. Acernese, K. Ackley, C. Adams, T. Adams, P. Addesso, R. Adhikari, V. Adya, *et al.*, Physical Review Letters **119**, 161101 (2017), arXiv:1710.05832.

[15] J. R. Smith, T. Abbott, E. Hirose, N. Leroy, D. MacLeod, J. McIver, P. Saulson, and P. Shawhan, Classical and Quantum Gravity **28**, 235005 (2011), arXiv:1107.2948.

[16] T. Isogai, L. S. Collaboration, V. Collaboration, *et al.*, in *Journal of Physics: Conference Series*, Vol. 243 (IOP Publishing, 2010) p. 012005.

[17] R. Essick, L. Blackburn, and E. Katsavounidis, Classical and Quantum Gravity **30**, 155010 (2013), arXiv:1303.7159.

[18] R. Biswas, L. Blackburn, J. Cao, R. Essick, K. A. Hodge, E. Katsavounidis, K. Kim, Y.-M. Kim, E.-O. Le Bigot, C.-H. Lee, *et al.*, Physical Review D **88**, 062003 (2013), arXiv:1303.6984.

[19] C. Messick, K. Blackburn, P. Brady, P. Brockill, K. Cannon, R. Cariou, S. Caudill, S. J. Chamberlin, J. D. Creighton, R. Everett, *et al.*, Physical Review D **95**, 042001 (2017), arXiv:1604.04324.

[20] S. A. Usman, A. H. Nitz, I. W. Harry, C. M. Biwer, D. A. Brown, M. Cabero, C. D. Capano, T. Dal Canton, T. Dent, S. Fairhurst, *et al.*, Classical and Quantum Gravity **33**, 215004 (2016), arXiv:1508.02357.

[21] N. J. Cornish and T. B. Littenberg, Classical and Quantum Gravity **32**, 135012 (2015), arXiv:1410.3835.

[22] A. Buonanno, B. R. Iyer, E. Ochsner, Y. Pan, and B. S. Sathyaprakash, Physical Review D **80**, 084043 (2009), arXiv:0907.0700.

[23] P. Ajith, S. Babak, Y. Chen, M. Hewitson, B. Krishnan, J. Whelan, B. Bruegmann, P. Diener, J. Gonzalez, M. Hannam, *et al.*, Classical and Quantum Gravity **24**, S689 (2007), arXiv:0704.3764.

[24] T. Li, W. Del Pozzo, S. Vitale, C. Van Den Broeck, M. Agathos, J. Veitch, K. Grover, T. Sidery, R. Sturani, and A. Vecchio, Physical Review D **85**, 082003 (2012), arXiv:1111.5274.

[25] T. G. Li, *Extracting physics from gravitational waves: Testing the strong-field dynamics of general relativity and inferring the large-scale structure of the Universe* (Springer, 2015).

[26] D. Sivia and J. Skilling, *Data analysis: a Bayesian tutorial* (OUP Oxford, 2006).

[27] G. Ashton, M. Hübner, P. D. Lasky, C. Talbot, K. Ackley, S. Biscoveanu, Q. Chu, A. Divakarla, P. J. Easter, B. Goncharov, *et al.*, The Astrophysical Journal Supplement Series **241**, 27 (2019), arXiv:1811.02042.